Evaluation of Mass Spectrometric Methods for Detection of the Anti-Protozoal Drug Imidocarb*

A.F. Lehner[1,†], J.A. Hitron[2], J. May[3], C. Hughes[4], R. Eisenberg[5], N. Schwint[6], D.P. Knowles[6], P. Timoney[4], and T. Tobin[4]

[1]Michigan State University, Diagnostic Center for Population & Animal Health, Lansing, Michigan 48910; [2]University of Kentucky, Graduate Center for Toxicology, Health Science Research Building, Lexington, Kentucky 40536-0305; [3]University of Kentucky, Environmental Research Training Laboratories, Raymond Building, Lexington, Kentucky 40506-0281; [4]University of Kentucky, Department of Veterinary Science, Maxwell H. Gluck Equine Research Center, Lexington, Kentucky 40546; [5]Frontier BioPharm, LLC, Richmond, Kentucky 40475; and [6]Washington State University, Department of Microbiology & Pathology, College of Veterinary Medicine, Pullman, Washington 99164

Abstract

Imidocarb [*N*,*N*'-bis[3-(4,5-dihydro-1H-imidazol-2-yl)phenyl]urea, $C_{19}H_{20}N_6O_1$, m.w. 348.41] is a symmetrical carbanilide derivative used to treat disease caused by protozoans of the *Babesia* genus. Imidocarb, however, is also considered capable of suppressing *Babesia*-specific immune responses, allowing *Babesia*-positive horses to pass a complement fixation test (CFT) without eliminating the infection. This scenario could enable *Babesia*-infected horses to pass CFT-based importation tests. It is imperative to unequivocally identify and quantify equine tissue residues of imidocarb by mass spectrometry to address this issue. As a pretext to development of sensitive tissue assays, we have investigated possibilities of mass spectrometric (MS) detection of imidocarb. Our analyses disclosed that an unequivocal mass spectral analysis of imidocarb is challenging because of its rapid fragmentation under standard gas chromatography (GC)–MS conditions. In contrast, solution chemistry of imidocarb is more stable but involves distribution into mono- and dicationic species, *m/z* 349 and 175, respectively, in acid owing to the compound's inherent symmetrical nature. Dicationic imidocarb was the preferred complex as viewed by either direct infusion-electrospray-MS or by liquid chromatography (LC)–MS. Dicationic imidocarb multiple reaction monitoring (MRM: *m/z* 175 → 162, 145, and 188) therefore offer the greatest opportunities for sensitive detection and LC–MS is more likely than GC–MS to yield a useful quantitative forensic analytical method for detecting imidocarb in horses.

Introduction

Imidocarb [*N*,*N*'-Bis[3-(4,5-dihydro-1H-imidazol-2-yl)phenyl]urea, $C_{19}H_{20}N_6O_1$, m.w. 348.41] is a symmetrical carbanalide derivative (Figure 1) widely used by veterinarians to treat babesiosis, a disease caused by ubiquitous erythrocyte-parasitizing protozoans of the *Babesia* genus (1). *Babesia* are transmitted to mammals by arthropod vectors, usually ticks, and accordingly animal cases of babesiosis can be found wherever competent tick vectors are present. Although babesiosis is most commonly observed in animals, human cases of babesial infections have also been reported (2).

Intramuscular or subcutaneous injection of imidocarb alters the ultrastructure of infective *Babesia* cells, resulting in condensation and clumping of the chromatin, dissolution of the nuclear envelope, and general vacuolization of the organism (3). Although imidocarb protects against clinical babesial infections, it also allows a subclinical level of babesial infection, so that immune responses develop, giving imidocarb a therapeutic prophylactic capability (4). It is because of this dual function that imidocarb remains a preferred treatment for babesiosis.

The United States Department of Agriculture (USDA) and its agencies the Animal and Plant Health Inspection Service

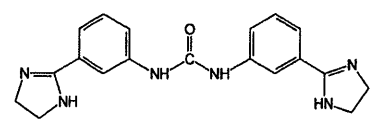

Figure 1. Imidocarb [$C_{19}H_{20}N_6O_1$, m.w. 348.41] structure, illustrating that it is a symmetrical bis-[4,5-dihydroimidazol-2-yl]-phenyl]-substituted urea.

* Published as paper #389 from the Equine Pharmacology, Therapeutics and Toxicology Program at the Maxwell H. Gluck Equine Research Center and Department of Veterinary Science, University of Kentucky. Published as Kentucky Agricultural Experimental Station Article #08-014-096 with the approval of the Dean and Director, College of Agriculture and The Kentucky Agricultural Experimental Station.

† Author to whom correspondence should be addressed: Andreas F. Lehner, Michigan State University, Diagnostic Center for Population & Animal Health, Lansing, MI 48910. Email: lehnera@dcpah.msu.edu.

(APHIS) and Foreign Agriculture Service (FAS), as well as international organizations such as the World Organization for Animal Health (OIE), provide strict guidelines for horse importation intended to prevent the spread of equine diseases such as piroplasmosis (5). Countries in which agriculturally significant *Babesia* species do not occur naturally, such as the United States and Australia, require *Babesia*-positive animals to be reported, quarantined, and re-exported or euthanized. Complement fixation tests (CFT) have more recently been superceded by competitive enzyme-linked immunosorbent assay (ELISA) tests for *B. caballi* and *T. equii* as the importation assays intended to screen out and disallow entry of infected animals. Imidocarb has been shown to suppress *Babesia*-related immune responses in some individuals to the extent that *Babesia*-infected horses appear negative on CFT importation tests (6). Therefore, the ability to unequivocally identify imidocarb residues in horses presented for equine piroplasmosis screening would be an important adjunct to piroplasmosis testing procedures.

Detection of imidocarb has typically involved solid-phase extraction and high-performance liquid chromatography (HPLC)–fluorescence detection (7), although liquid–liquid extraction methods have been reported in the literature (8,9). This paper advocates development and use of mass spectrometric (MS) techniques for imidocarb detection because of the chemical specificity of such techniques as well as the capacity to identify any metabolites or breakdown products. Complexities exist in using such methods as are described herein, and a plan for circumventing pitfalls is discussed.

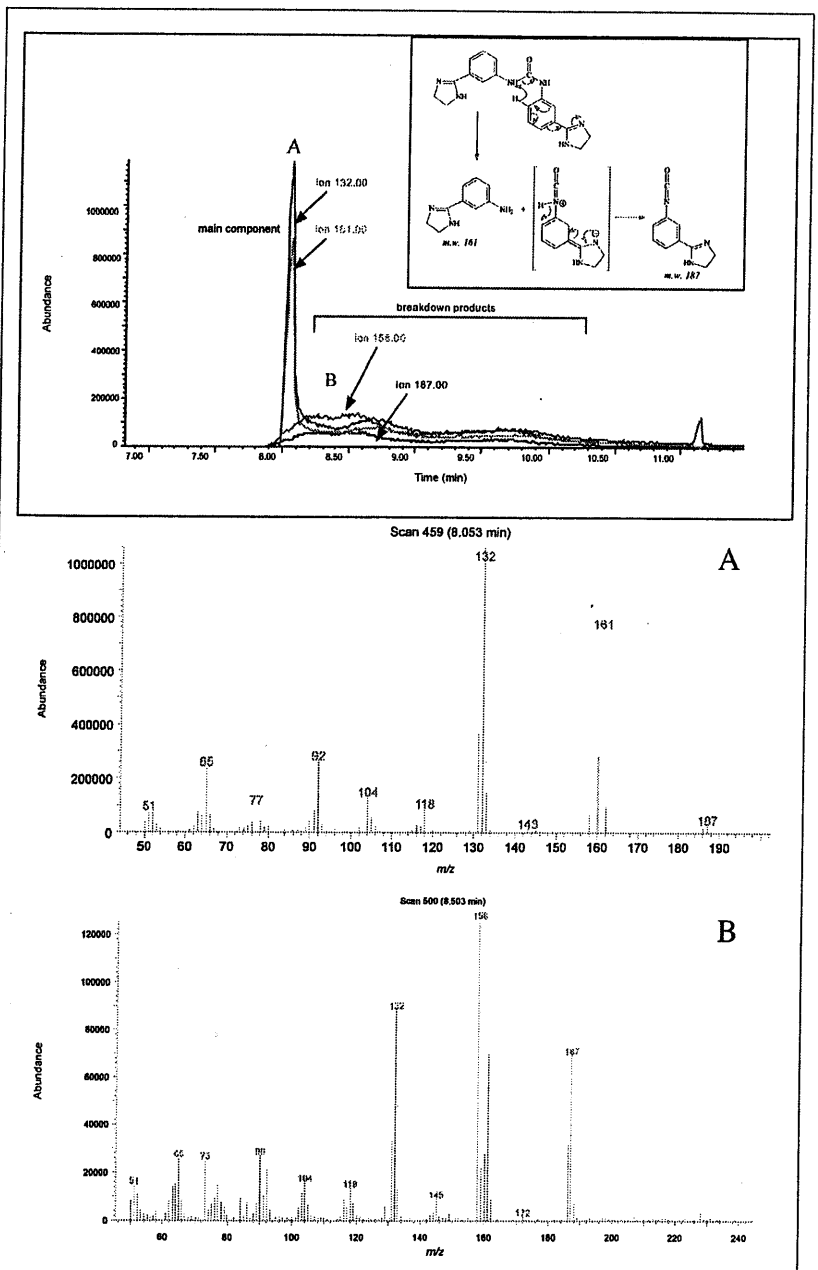

Figure 2. GC–MS of imidocarb dissolved at 20 ng/µL in dichloromethane/*N*,*N*-dimethylformamide (3:1). Ion chromatography shows principal components (*m/z* 187, 158, 161, 132), and inset shows likely reaction scheme to generate the principal components of m.w. 161 and 187 (top). Background-subtracted mass spectra of principal components A (8.1 min) and B (8.5 min) as labeled in the top figure (bottom).

Materials and Methods

Chemicals

Imidocarb was available as a dipropionate salt from Sigma-Aldrich (St. Louis, MO) with the formula $C_{25}H_{32}N_6O_5$ molecular weight (m.w.) 496. The imidocarb portion is $C_{19}H_{20}N_6O_1$ with m.w. 348.

Gas chromatography (GC)–MS conditions

Examination by GC–MS was carried out on an Agilent 5890/5970 instrument. The GC column was a J&W (Agilent, Santa Clara, CA) DB-5 MS column (10 m × 0.25 mm, 0.25-µm film thickness) operated in the splitless mode with 1 mL/min helium flow. The GC oven temperature was programmed as follows: 70°C for 2 min, then increased to 280°C at 20°C/min, and held at 280°C for 10 min. The injector was kept at 220°C, and the transfer line was 280°C. Data were collected following a 1-µL injection as follows: for GC–MS scanning experiments, the *m/z* 50–700 mass range was scanned at 1.19 scans/s.

Pentafluoropropionic anhydride (PFPA) reaction of imidocarb

Imidocarb (10 µg) was reacted with 50 µL pentafluoropropionic anhydride (PFPA)

(Pierce Chemical, Rockford, IL) with 1 µL triethylamine (Aldrich Chemical, Milwaukee, WI) as catalyst for 45 min at 60°C (10).

Triple-stage quadrupole MS

The Varian LC–MS–MS (Varian, Palo Alto, CA) consisted of two Varian ProStar 210 LC pumps connected to a Varian 1200L tandem quadrupole MS–MS system. The MS parameters were optimized while infusing 10 µg/mL of imidocarb dissolved in acetonitrile/water (1:1). The MS was operated in positive ion mode with the electrospray ionization (ESI) probe installed. Nitrogen was used as both drying and nebulizing gas. The drying gas temperature was set at 300°C at 20 psi, and the nebulizing gas was set at 50 psi. The needle voltage was set at 5000 V, the shield voltage at 600 V, and capillary voltage at +30 V. The electron multiplier was set at 1700 V. Collision gas (argon) and collision energy were adjusted for collisionally induced dissociation (CID) in the central hexapole by optimizing settings for the second quadrupole; typical settings: the collision gas was set at 2 mTorr and collision energy was set at –20 eV.

Imidocarb detection by LC–MS–MS

On dissolution in water/acetonitrile + 0.03% formic acid (95:5), imidocarb readily produced both a monoprotonated *m/z* 349 $[M+H]^+$ ion and a diprotonated *m/z* 175 $[M+2H]^{2+}$ ion. Detection of these forms was carried out on the Varian LC–MS–MS equipped with a Phenomenex (Torrance, CA) 4-mm × 2-mm phenylpropyl guard column and Phenomenex Luna phenyl-hexyl column (30 mm × 1 mm, 30-µm particle size). Gradient chromatography with the HPLC–ESI(+)-MS–MS involved two solvent systems, A = water/acetonitrile + 0.03% formic acid (95:5) and B = acetonitrile + 0.03% formic acid, flowing at 0.15 mL/min throughout. These were as varied as 100% A from 0 to 3 min, varying to 10% A, 90% B by 15 min, and then resetting to 100% A by 19 min.

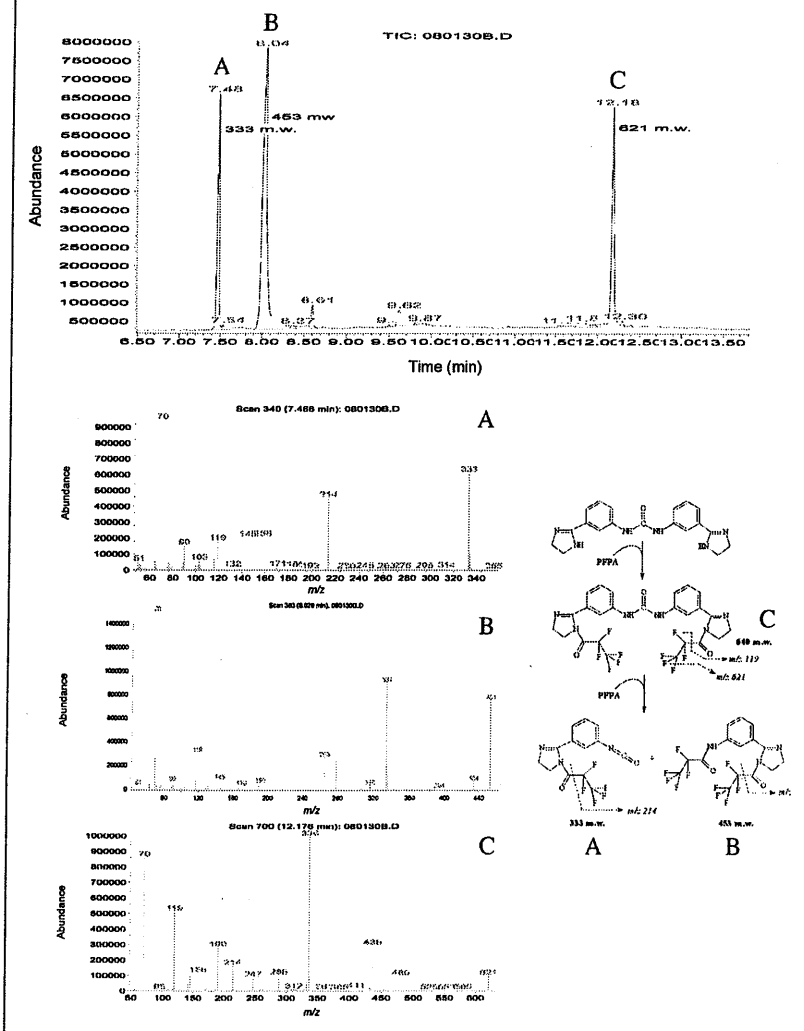

Figure 3. Imidocarb derivatization. GC–MS of imidocarb (~10 µg) reacted with 50 µL pentafluoropropionic anhydride (PFPA) + 1 µL triethylamine (45 min at 60°C) and diluted 1:10 into dichloromethane prior to injection of 1 µL (top); EI-mass spectra of principal PFPA-generated products, with labels A–C corresponding to peaks in chromatogram at retention times of 7.5, 8.0, and 12.2 min (bottom left); and pathway from imidocarb to the 640 m.w. diacetyl derivative, and its thermal decomposition in the presence of excess derivatizing agent to 333 and 453 m.w. species as shown (bottom right). Dotted lines indicate cleavages responsible for the major species seen on EI-MS.

Results and Discussion

GC–MS analysis of imidocarb

GC–MS analysis of imidocarb revealed a major component and a series of complex overlapping thermal breakdown products as shown in the ion chromatograms of Figure 2. This figure also includes the electron impact (EI)-mass spectra of the principal components, a 161 m.w. component that elutes as a relatively sharp peak at 8.05 min and a 187 m.w. principal component nestled among poorly chromatographing breakdown products. A reaction pathway illustrates thermally induced intramolecular rearrangement that offers an interpretation of these MS results. The 161 m.w. amine appears to be stable because of its clean chromatography. In contrast, the 187 m.w. isocyanate structure can be expected to react with traces of water to generate an unstable carbamate, or with amines to generate N,N-disubstituted ureas (11).

PFPA derivatization of imidocarb supports the Figure 2 scheme for thermal degradation into isocyanate and carbamate fragments. Reaction can be expected between free imidazole imino N-H groups and pentafluoropropyl acyl groups to give

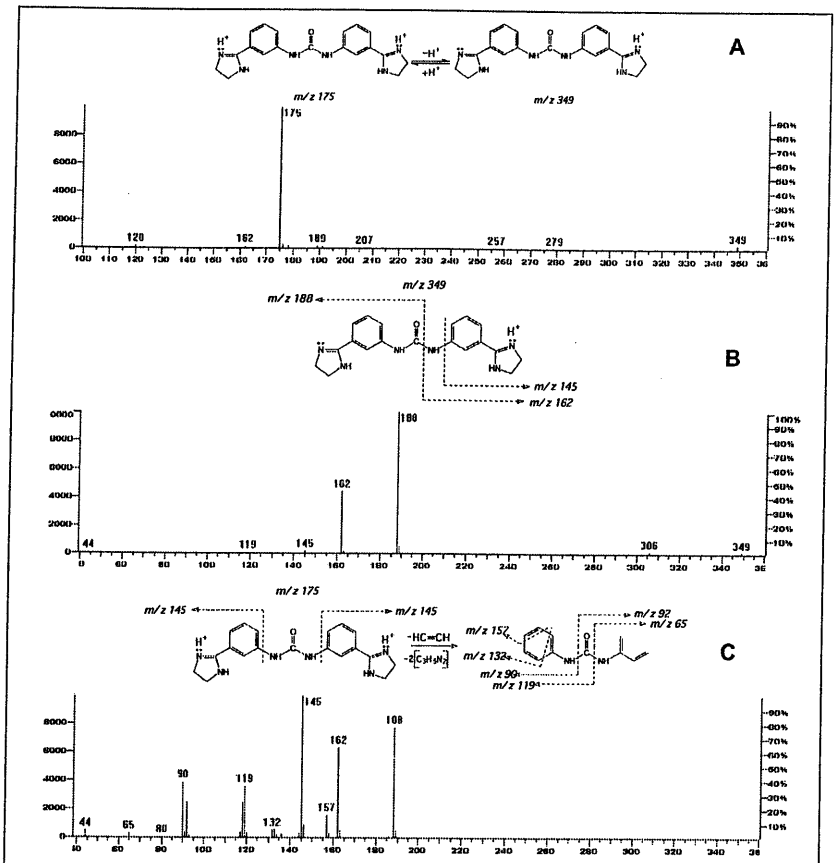

Figure 4. Imidocarb examined by ESI-MS. Imidocarb 10 µg/mL examined by direct infusion-full scan in water/acetonitrile, 1:1 from *m/z* 100 to 400 (A). Structures show origins of principal peaks at *m/z* 175 and 349 as di- and mono-cationic species; *m/z* 349 daughter ions by ESI full scan from *m/z* 10 to 400 at –25 collision energy (B). Structures show cleavage of monocationic imidocarb to give principal species; *m/z* 175 daughter ions by ESI full scan from *m/z* 10 to 400 at –25 collision energy. Structures show cleavage and fragmentations of dicationic imidocarb to give principal species (C).

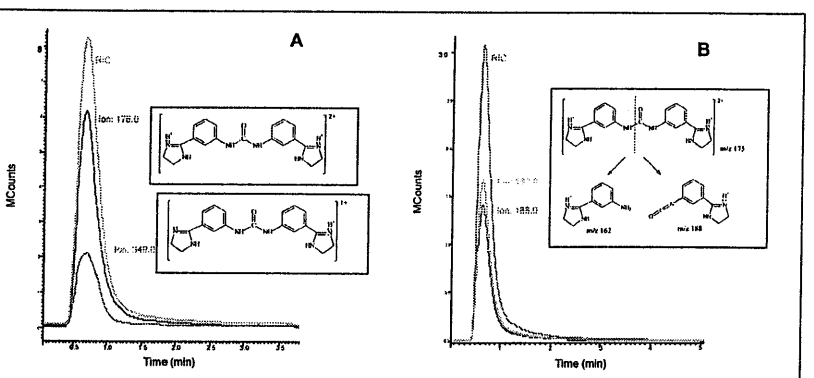

Figure 5. Imidocarb LC–MS. Selected ion monitoring (SIM) of the imidocarb 100 ppb standard for ions *m/z* 349.0 and 175.0. Both ions are present, but *m/z* 175 is more plentiful and therefore more suited for greater sensitivity (A). Multiple reaction monitoring (MRM) analysis of the imidocarb 100 ppb standard for fragmentations *m/z* 175 →162 and *m/z* 175 → 188 (B). HPLC conditions: 10%ACN/90% (0.05% formic acid, aq) to 90%ACN/10% (0.05% formic acid, aq) over 12 min on the Phenomenex 1-mm x 30-mm, 3-u Luna phenyl-hexyl column. Electrospray ionization at 12 V collision energy with argon collision gas. Inset figures illustrate complexation with protons to give mono- or dicationic species (A) and cleavage of the dicationic species to generate *m/z* 162 and 188.

stable amido products. Figure 3 shows GC–MS analysis of such a reaction product, indicating three major peaks, C being the intact imidocarb reaction product and A & B being the thermal decomposition products analogous to results of Figure 2. Figure 3 includes the EI-mass spectra of the principal GC peaks with expanded data acquisition from *m/z* 50 to 750. The Figure 3 sidebar offers an interpretation of these results, in which an expected 640 m.w. diacetylated product loses a single fluorine atom to explain the appearance of a 621 m.w. species. Presumably the pattern of products arises from thermal degradation of imidocarb in the GC injector port followed by rapid immediate reaction with excess PFPA reagent; degradation of intact imidocarb-PFPA products is also a possibility. The pattern of GC–MS-identified products was further supported by reaction with the similar acylating reagent heptafluorbutyric anhydride (HFBA) which generated thermal breakdown products of molecular weights 383 and 553, that is, the monoacylated isocyanate and diacylated amine, respectively (data not shown).

In attempts to alleviate thermally induced degradation, the injector port temperature and/or the column oven temperature were varied; these efforts provided no improvement of the observed outcome (data not shown). Furthermore, derivatization of imidocarb with methyl groups or TMS groups provided complex, difficult-to-interpret mixtures of products (data not shown).

In conclusion, GC–MS screening of relevant derivatized extracts could form the basis of an imidocarb qualitative screen, but distribution among three or more product peaks is unsatisfactory, particularly if quantitation were desired. GC–MS screening for PFPA-derivatized products, particularly peak C in Figure 3, could be an adequate and sensitive screen with application of MS or even electron capture detection enabled by the presence of 10 fluorine atoms. Thermal instability and rearrangements nevertheless motivated us to examine ESI-MS as an alternative detection mechanism.

LC–MS analysis of imidocarb

ESI$^+$-triple-stage quadrupole MS was investigated as an alternative detector with introduction by direct infusion of

imidocarb in a 95:5 water/acetonitrile, 0.03% formic acid solution, which yielded the spectrum seen in Figure 4A. The significant *m/z* 175 peak and the relatively minor *m/z* 349 peak are interpreted as dicationic and monocationic species arising by complexation of the 348 m.w. imidocarb in solution with two or one proton, respectively, consistent with the symmetrical structure of imidocarb and illustrated schematically in Figure 4A.

The *m/z* 349 monocationic imidocarb species gave straightforward product ions as shown in the middle panel of Figure 4 with principal fragmentations arising in the central urea functionality as shown schematically to give *m/z* 162 and 188 species, along with the minor *m/z* 145. Note that the *m/z* 162 and 188 species correspond to cleavages occurring in GC–MS as well (Figure 2). The dicationic structural interpretation for the *m/z* 175 fragment was supported by examination of its product ions (Figure 4C), shown at the equivalent collision energy as that for *m/z* 349. One clear indicator of the doubly charged property is the ability of the *m/z* 175 species to generate higher m.w. daughter ions, particularly *m/z* 188. Note the commonality of product ions between *m/z* 349 and 175 species, particularly *m/z* 188, 162, and 145. The structural interpretation in Figure 4C indicates doubled chances for generation of *m/z* 145, accounting for the significant increase in this ion. *m/z* 175 product ions indicate an additional layer of fragmentation events to *m/z* 157, 132, 119, 92, 90, and 65. Complexation with two protons apparently opens routes to these fragments by release of neutral imidazolines plus cleavage of a phenyl ring to release ethylene to give an unstable intermediate that one can surmise as being responsible for these fragments, as shown in Figure 4C.

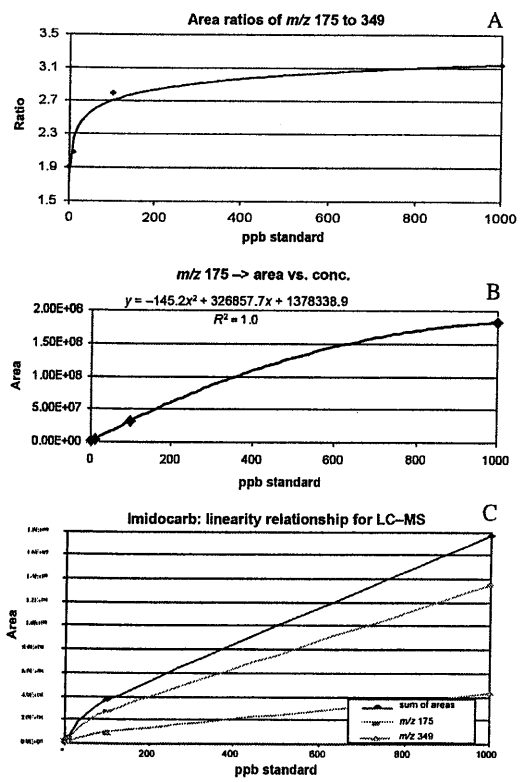

Figure 6. A: Biphasic dependence of [*m/z* 175]/[*m/z* 349] area ratio on compound concentration (ppb of standard). B: Curvilinearity of *m/z* 175→162 area plotted relative to concentration (ppb of imidocarb standard), including polynomial formula and coefficient of determination, R^2. C: Overall curvilinearity of *m/z* 175 and 349 areas plotted relative to concentration (ppb of imidocarb standard), including a plot of the summed (*m/z* 175 + *m/z* 349) areas.

The much greater intensity of *m/z* 175 (Figure 4A) suggests this ion to be the preferred species for sensitive ESI+ ionization and detection following HPLC. Figure 5A indicates significantly greater yield of the *m/z* 175 ion versus *m/z* 349 based on selected ion monitoring (SIM) of these overlapping imidocarb species seen by HPLC. Figure 5B demonstrates multiple reaction monitoring (MRM) detection of *m/z* 175-generated species *m/z* 162 and 188 under the same HPLC conditions. Structural inserts in Figure 5 remind of the origin of each of the labeled species.

Repeating the experiment with full scan acquisition across the imidocarb peak at 0.8-min retention time and examination of its ESI-mass spectrum revealed a difference from the direct infusion mass spectrum of Figure 4A, namely much greater *m/z* 349 intensity (data not shown). Specifically, the *m/z* 349 intensity was 35% that of the *m/z* 175 base peak, in contrast to its much smaller size on direct infusion on the order of 5% as seen in Figure 4A. This difference may reflect ion-suppressive effects of solvent arising, for example, from the significantly higher acetonitrile concentration present during direct infusion than during HPLC. This contention can be proven by repeated infusion of imidocarb at a set concentration under conditions of increasing concentration of acetonitrile or other mobile phase solvents or components while also monitoring imidocarb response in terms of area or intensity. In any case, a deuterated imidocarb internal standard can be prepared for future work to alleviate any deleterious effects of suppression by solvent components and by application of quantitation by isotope dilution MS (12–15).

The apparent preference for dicationic charge distribution in imidocarb at least in the gas phase of the ESI source if not also in solution is underscored by the greater than twofold area response for *m/z* 175 versus *m/z* 349 (Figure 5A). This differs markedly from cases in which bis-quarternary amines with highly electron-deficient dicationic cores stabilize by dissociation, transfer of an electron, loss of a proton, or formation of clusters (16). Imidocarb is nonetheless not immune to gas phase intermolecular effects such as intermolecular complexation or proton transfer. Examination of a series of unextracted imidocarb standards demonstrates an interesting aspect of the relationship of signal response to overall imidocarb concentration. Specifically, Figure 6A indicates a biphasic dependence of the amount of *m/z* 175 area on overall imidocarb concentration, with a rapid rise in *m/z* 175/*m/z* 349 area ratio at lower values, followed by a more gradual rise in the relationship above 100 ppb. Nevertheless, a dependable curvilinear relationship between unextracted standards and concentration can be elaborated on the basis of the *m/z* 175 → 162 MRM area determinations which could be fit to the polynomial equation

area = $-145.2x_{(\text{conc. ppb})}^2 + 326857x_{(\text{conc. ppb})} + 1378339$ (Figure 6B). This could offer the basis for a quantitative LC–MS–MS imidocarb method; however, it may ultimately be more appropriate to take *m/z* 349 daughter ions into account as well for greater accuracy and sensitivity, particularly in light of the overall curvilinear response of both parent *m/z* 175 and 349 ions as seen for standards in Figure 6C.

Conclusions

GC–MS analysis of underivatized imidocarb revealed complex patterns of products arising principally from intramolecular cleavage.

PFPA and HFPA derivatization for GC–MS support the interpretation of principal cleavage to isocyanate and carbamate fragments.

ESI^+-MS revealed that imidocarb readily distributes itself into mono- and dicationic species when dissolved in acid solution.

Dicationic imidocarb MRM (*m/z* 175 → 162, 145, and 188) offer the greatest opportunities for sensitive detection while avoiding the thermal instabilities seen in GC–MS.

Because of the inherent symmetrical nature and thermal instability of imidocarb, LC–MS is more likely than GC–MS to yield a useful quantitative forensic analytical method for detecting imidocarb or possibly even metabolites thereof in horses.

Validation of an imidocarb method based on the listed considerations and intended for examination of biological specimens is the goal of future papers on this topic.

Acknowledgments

This work was made possible by research support from The National Horsemen's Benevolent and Protective Association and the Alabama; Arizona; Arkansas; Canada; Charles Town, WV; Florida; Iowa; Kentucky; Louisiana; Michigan; Minnesota; Nebraska; Ohio; Oklahoma; Ontario, Canada; Oregon; Pennsylvania; Tampa Bay Downs, Florida; Texas; Washington State; and West Virginia Horsemen's Benevolent and Protective Associations.

References

1. H. Mehlhorn and E. Shein. The piroplasms: life cycle and sexual stages. *Adv. Parasitol.* **23:** 37–103 (1984).
2. B.L. Herwaldt, D.H. Persing, E.A. Precigout, W.L. Goff, D.A. Mathieson, P.W. Taylor, M.L. Eberhard, and A.F. Gorenflot. A fatal case of babesiosis in Missouri: identification of another piroplasm that infects humans. *Ann. Intern. Med.* **124:** 643–650 (1996).
3. C.F. Simpson and F.C. Neal. Ultrastructure of *Babesia equi* in ponies treated with imidocarb. *Am. J. Vet. Res.* **41:** 267–271 (1980).
4. H.J. Vial and A. Gorenflot. Chemotherapy against babesiosis. *Vet. Parasitol.* **138:** 147–160 (2006).
5. Committee on Foreign and Emerging Diseases of the United States Animal Health Association. *Foreign Animal Diseases*, 7th ed. Boca Publications Group, Boca Raton, FL, 2008.
6. C.M. Butler, A.M. Nijhof, J.H. van der Kolk, O.B. de Haseth, A. Taoufik, F. Jongejan, and D.J. Houwers. Repeated high dose imidocarb dipropionate treatment did not eliminate *Babesia caballi* from naturally infected horses as determined by PCR-reverse line blot hybridization. *Vet. Parasitol.* **151:** 320–322 (2007).
7. J.A. Tarbin and G. Shearer. High-performance liquid chromatographic determination of imidocarb in cattle kidney with cation-exchange clean-up. *J. Chromatogr.* **577:** 376–381 (1992).
8. N.G. Coldham, A.S. Moore, M. Dave, P.J. Graham, S. Sivapathasundaram, B.G. Lake, and M.J. Sauer. Imidocarb residues in edible bovine tissues and in vitro assessment of imidocarb metabolism and cytotoxicity. *Drug Metab. Dispos.* **23:** 501–505 (1995).
9. G. Crescenzo, O.R. Lai, C. Belloli, G. Sasso, and P. Ormas. Validation of analytical methods for the determination of imidocarb in tissues and milk of cattle, sheep and goats. *Ital. J. Food Sci.* **14:** 99–111 (2002).
10. Acylation Derivatization Reagents. Pierce Biotechnology, Inc.: Rockford, IL, 2004.
11. G. Raspoet, M.T. Nguyen, M. McGarraghy, and A.F. Hegarty. Experimental and theoretical evidence for a concerted catalysis by water clusters in the hydrolysis of isocyanates. *J. Org. Chem.* **63:** 6867–6877 (1998).
12. B.A. Way, D. Stickle, M.E. Mitchell, J.W. Koenig, and J. Turk. Isotope dilution gas chromatographic–mass spectrometric measurement of tricyclic antidepressant drugs. Utility of the 4-carbethoxyhexafluorobutyryl derivatives of secondary amines. *J. Anal. Toxicol.* **22:** 374–382 (1998).
13. G. Singh, V. Arora, P.T. Fenn, B. Mets, and I.A. Blair. A validated stable isotope dilution liquid chromatography tandem mass spectrometry assay for the trace analysis of cocaine and its major metabolites in plasma. *Anal. Chem.* **71:** 2021–2027 (1999).
14. S.S.-C. Tai and M.J. Welch. Determination of 11-nor-9-tetrahydrocannabinol-9-carboxylic acid in a urine-based standard reference material by isotope-dilution liquid chromatography–mass spectrometry with electrospray ionization. *J. Anal. Toxicol.* **24:** 385–389 (2000).
15. S.A. White, A.S. Kidd, and K.S. Webb. The determination of lysergide (LSD) in urine by high-performance liquid chromatography–isotope dilution mass spectrometry (IDMS). *J. Forensic Sci.* **44:** 375–379 (1999).
16. C.A. Schalley, C. Verhaelen, F.-G. Klärner, U. Hahn, and F. Vögtle. Gas-phase host-guest chemistry of dendritic viologens and molecular tweezers: a remarkably strong effect on dication stability. *Angew. Chem. Int. Ed. Engl.* **44:** 477–480 (2005).

Manuscript received August 12, 2010;
revision received October 18, 2010.